ADVANCES IN MATERIALS SCIENCE, Vol. 21, No. 4 (70), December 2021

DOI: 10.2478/adms-2021-0025

Dhanesh G. Mohan[1*], S. Gopi[2], Jacek Tomków[3], Shabbir Memon[4]

[1]*Institute of Materials Joining, Shandong University, Jinan, China*
[2]*Department of Production Engineering, Government College of Technology, Coimbatore, Tamilnadu, India*
[3]*Faculty of Mechanical Engineering and Ship Technology, Gdańsk University of Technology, Poland*
[4]*Department of Mechanical Engineering, Wichita State University, Kansas, USA*

** dhaneshgm@gmail.com*

ASSESSMENT OF CORROSIVE BEHAVIOUR AND MICROSTRUCTURE CHARACTERIZATION OF HYBRID FRICTION STIR WELDED MARTENSITIC STAINLESS STEEL

ABSTRACT

This study examined the effect of induction heating on the microstructure and corrosion characteristics of hybrid friction stir welded AISI 410 stainless steel. Five joints have been produced with different friction stir welding parameters like welding speed, spindle speed, plunge depth, and induction power. Their microstructures were evaluated using a scanning electron microscope, and chemical composition was examined using energy-dispersive X-ray spectroscopy (EDX). The rate of corrosion was found out via the weight loss method in a 1 M HCL solution. The hybrid friction stir welding method used for this work is induction assisted friction stir welding; the results show that this method could produce sound AISI 410 stainless steel Joints. The experiment results show that the joint made at a spindle speed of 1150 rpm, welding speed 40 mm/min, plunge depth 0.5 mm, and in-situ heat by induction 480°C show a better corrosion resistance property with a fine grain structure.

Keywords: *hybrid welding; induction heating; stainless steel; friction stir welding; corrosion; microstructure*

INTRODUCTION

As a predominant engineering material, stainless steel has many industrial applications due to its high strength and corrosion resistance [1]. For instance, ferritic stainless steel is used for automobiles and kitchen applications due to its malleability. Austenitic stainless steel is widely used due to its superior corrosion resistance properties in acidic environments. The martensitic stainless steels are magnetic and have a high strength compared to ferritic and austenite stainless steels [2,3]. These stainless steel types are mainly used for making propeller blades, mixer blades, pumps and valves [4]. Compared with austenitic and ferritic steels, martensitic steel is difficult to weld due to its high hardness and its prone to hydrogen cracking, and these problems need to be addressed well.

In this current scenario, due to the requirement of high strength and eco-friendly joining

methods, there has been a growing interest in new metal joining methods like welding [5]. For example, Friction Stir Welding (FSW), brought up by The Welding Institute (TWI), the U.K., is a solid-state welding technique that eradicates the welding defects such as gas porosity, cracking and distortion which happens in conventional fusion welding [6−8]. However, much concentration has also been given for welding hard structural metals like steel and its alloys with high melting points [9−12]. Moreover, various studies need to be conducted on welding dissimilar metals and alloys with different melting points with friction stir welding [13,14].

Numerous experiments were conducted on FSW for joining soft metals like aluminium and its alloys; the experiments show that this solid-state welding method is accurate for joining soft metals [15–17]. While applying FSW to hard metals like steel, the tool is damaged easily, and the joint strength gained is low due to the insufficient heat produced by the tool pin and shoulder [18,19]. The available solution to overcome these issues is Hybrid Friction Stir Welding. The Hybrid Friction Stir Welding means an additional heating source is attached to the FSW for in situ heating process [20–22]. The investigations on hybrid FSW show that it can improve joint strength and enhance the tool life [23−25]. The additional heating sources selected for in situ heating are induction heating, laser heating, arc heating and resistance heating. The previous investigations reveal that the most predominant parameters influencing the mechanical properties and corrosion resistance property of the Hybrid FSW joints are welding speed, spindle speed and additional heat input [26]. Besides, the remaining parameters also influence the joint strength, but this is negligible compared to the above parameters.

More recently, the heat source selected for the hybrid FSW process was the induction heating and laser heating methods. These two methods provide quick localized heating with high accuracy; laser heating can heat metals much quicker than induction heating. The limitations of laser heating compared to induction heating are that it is very costly and cannot heat the metal volumetrically. Moreover, laser handling is much more complex when compared to induction heating [27,28]. Among these heating sources, induction heating is economical and applicable for in situ heating purposes. AISI 410 martensitic stainless steel is widely used in marine applications, especially for turbine blades. So, in this research, an Induction Assisted Friction Stir Welding (IA-FSW) method was adopted to weld AISI 410 martensitic stainless steel and investigate the effect of in-situ induction heating on the corrosive behaviour (by 3 hours and 24 hours weight loss method in 1 M HCL solution) and microstructural changes in the welded region.

EXPERIMENTAL

A 4 mm AISI 410 stainless steel plate of 100 mm × 150 mm with the chemical composition (compositions as provided in the materials certificate (as per ASTM standards) provided by the metal supplier) given in Table 1 were chosen for IA-FS Welding. The IA-FSW setup is presented in Figure 1. The mating surfaces were cleaned with acetone solution and dried to configure the butt joint. A tungsten carbide shank (grade–C6) was machined using the wire-cut electric discharge machining process (shown in Figure 2) to a hexagonal profile pin (2 mm pin length, 3mm pin diameter and 12 mm flat shoulder) for conducting the IA-FSW process [29−31]. The in-situ heating was done through an induction-heating coil diameter of 12 mm; the induction coil diameter is identical to the tool shoulder dimension. This coil was made using a copper tube of 2 mm external and 1.8 mm internal diameters, given in Figure 3. While performing the induction in-situ heating process, cold water will flow through the heating coil, preventing overheating. Different samples were welded based

on different spindle speed, welding speed, plunge depth, and induction power. Welding parameters and ranges conducting the IA-FSW experiment were given in Table 2. The induction heat input in terms of W and its corresponding temperature in ºC are also furnished in Table 2. The temperature related to each induction power input was identified using a thermal imager.

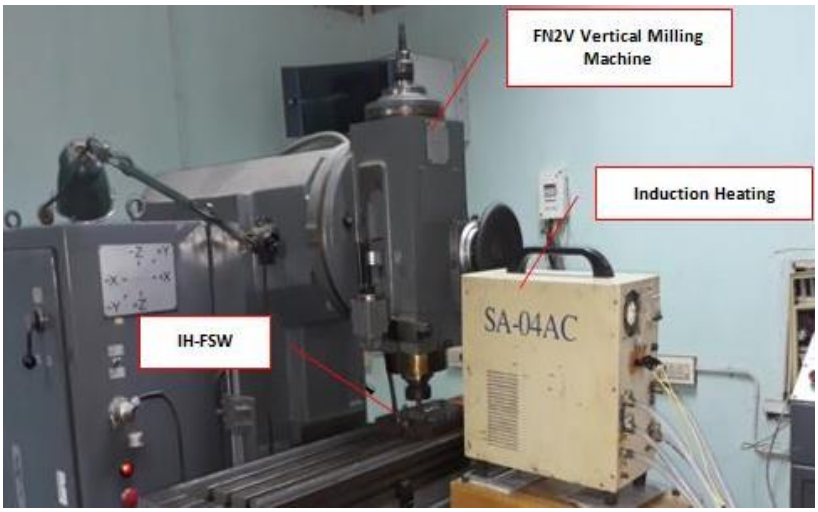

Fig. 1. IA-FSW setup

Table 1*. Chemical compositions of AISI 410 stainless steel in wt%*

Carbon	Manganese	Silicon	Phosphorus	Sulphur	Chromium	Nickel	Iron
0.15 %	1%	1%	0.04%	0.03%	12.5%	0.75%	Remaining

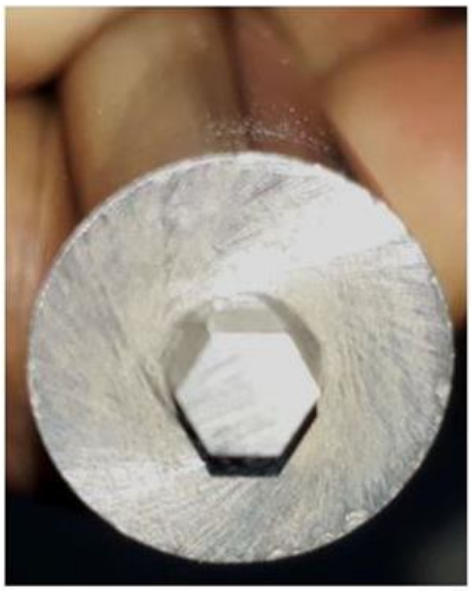

Fig. 2. IA-FSW sample tool

Fig. 3. Induction heating coil

Table 2. *IA-FSW Parameters*

Sample number	S1	S2	S3	S4	S5
Spindle Speed (rpm)	850	1000	1150	1300	1450
Welding Speed (mm/min)	25	30	35	40	45
Plunge Depth (mm)	0.3	0.4	0.5	0.6	0.7
Induction Power (W) with corresponding temperature	30 (300ºC)	35 (390ºC)	40 (480ºC)	45 (570ºC)	50 (660ºC)

The IA-FSW joints were cut into a dimension of 10 mm × 10 mm × 3 mm, including the welded region cross-sections and then polished using 200 to 1000 grade silicon carbide sanding papers. Kalling's No.2 solution (12 g CuCl2 + 20 mL HCL + 225 mL C_2H_5OH) was used as an etching solution for microstructure evaluation [32,33]. An optical microscope took the bead geometry, and the microstructure evaluations were conducted with the aid of a Scanning Electron Microscope (SEM) having an Energy Dispersive X-ray Spectroscopy (EDX) analyzer for finding out the composition of elements in the welded region [34]. IA-FSW's influence on the corrosive behaviour of AISI 410 welded joints was analyzed by 3 hours and 24 hours weight loss method in 1 M HCL solution.

RESULTS AND DISCUSSION

Corrosion test result

The IA-FSW joints' corrosion behaviour was analyzed through three hours and twenty-four hours weight loss methods, and the test was conducted using 1M HCL (92 ml distilled H2O + 8 mL HCL) solution. For each time periods (3hr and 24hr), two specimens were used to conduct the experiments, and the average value was taken. With the corrosion rate equation's aid, the corrosion rate that happens to the joints was found out.

$$\text{Corrosion Rate (C. R.)} = \frac{(\text{Weight loss (g)} \times \text{K})}{\left(\text{Alloy Density}\left(\frac{\text{g}}{\text{cm}^3}\right)\right) \times (\text{Area Exposed(A)} \times \text{Exposure time (hr)})}$$

In the corrosion rate equation, the K stands for corrosion rate constant called K-factor; the value of K is 8.75 ×104. The density of AISI 410 martensitic stainless steel is 7.80 g/cm3, where the area exposed (A) is 100 mm2 and the time of exposure are three hours and twenty-four hours. The weight loss in grams and the corrosion rate (C.R.) in mm/year for the corrosion weight loss test were provided in Table 3.

The two different times helps to predict the corrosion rate more accurately. The parameter combination like spindle speed 1150 rpm, welding speed 40 mm/min, plunge depth of 0.5 mm and an induction heat input of 480ºC at 40 W power shows the highest corrosion resistance property. The corrosion rate gained for sample S3 has the highest corrosion resistance ability; the rate of corrosion for S3 is 1.80600 mm/year for the 3-hour test and 1.82017 mm/year for the 24-hour test. Furthermore, this rate of corrosion is much higher compared to the base metal. Homogenous grains were gained in the welded region, enhancing the corrosion resistance property of the joint [35-36]. Moreover, it was documented by the literature [37] that grain refinement increases the corrosion resistance of stainless steel. The homogenous refined grains formed in the weld region can resist the bilayer corrosion film

formed on the weld surface [38,39]. The bilayer corrosion film gives maximum destruction to the weldment's heat affected zone due to its improper non-homogenous grain structures.

Table 3. *Weight loss corrosion test results*

	3 hours		24 Hours	
Sample Numbers	Weight loss (g)	Average rate of Corrosion (mm/year)	Weight loss (g)	Average rate of Corrosion (mm/year)
S1	0.05076	1.89793	0.42150	1.97015
S2	0.05072	1.89658	0.42120	1.96875
S3	0.04097	1.80600	0.41010	1.82017
S4	0.04124	1.81591	0.42550	1.88885
S5	0.05095	1.90511	0.42310	1.97763

The experiment reveals that while increasing the spindle speed and in situ heating, the joint's corrosion resistance property enhanced up to the point where the spindle speed is 1150 rpm and in situ heating temperature of 480ºC; after reaching that point, the corrosion rate of the joints was increased. It is shown in the graph provided in figure 4. The welding speed has less influence on the rate of corrosion compared with the other parameters.

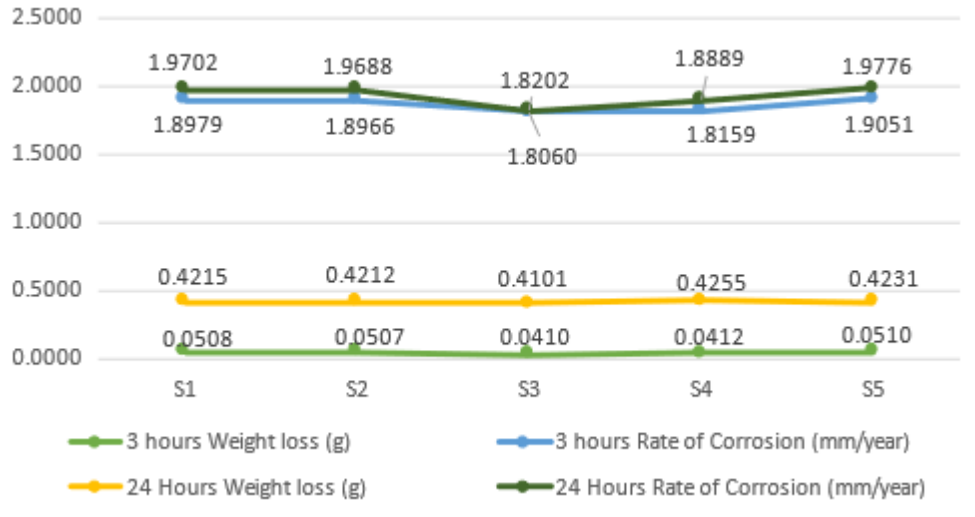

Fig. 4. Rate of corrosion graph for 3hr and 24hr tests

Macro and microstructure analysis

Figure 5 shows the IA-FSW specimen's bead geometry, a cross-sectional area of the weld joint. By using an optical scanner, the image was taken. Except for sample S1, all the other pieces were welded successfully, and sample S1 was damaged due to the formation of a tunnel in the welded region [40-43]. The insufficient material flow causes the formation of a tunnel in the stir zone. Porosity may also happen in this region due to the low spindle speed

[44]. The image clearly shows the nugget zone where the maximum stir was happened by the tool pin. An onion ring formation is happening in the nugget zone [45,46]. This onion ring formation is due to the stirring of metals from the two metal plates. Besides, sound defect-free welding was obtained through the IA-FSW method.

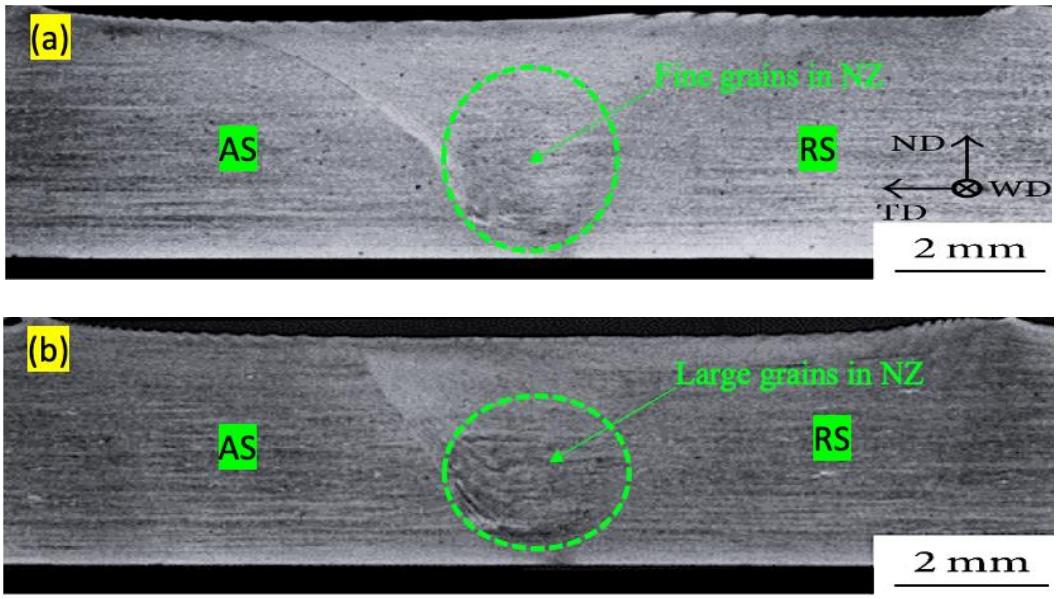

Fig. 5. Bead geometry of the IA-FSW specimen (a) Sample – 3 (b) Sample – 4

The homogenous grain structure was gained for sample S3 while comparing it with the other samples. This homogenous structure was achieved due to the proper spindle speed, welding speed and in situ heat input. The sample S4 is also acceptable, but the grain structure gained was not homogenous [47-50]. The increase in the values of parameters initially increased the joints' corrosion resistance, and later it decreased after attaining the spindle speed of 1150 rpm and welding speed of 40 mm/min.

The micrographs were taken from the different areas of the IA-FSW joint sample 3 (S3). The heat-affected zone (HAZ) was shown in Figure 6, the thermomechanical affected zone (TMAZ) was shown in Figure 7, and the stir zone (SZ) was shown in Figure 8.

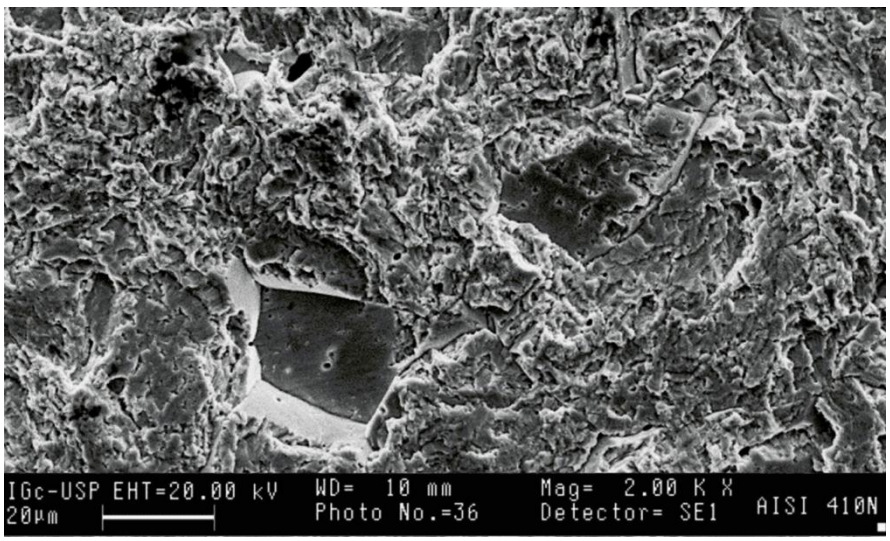

Fig. 6. Micrograph of HAZ of S3

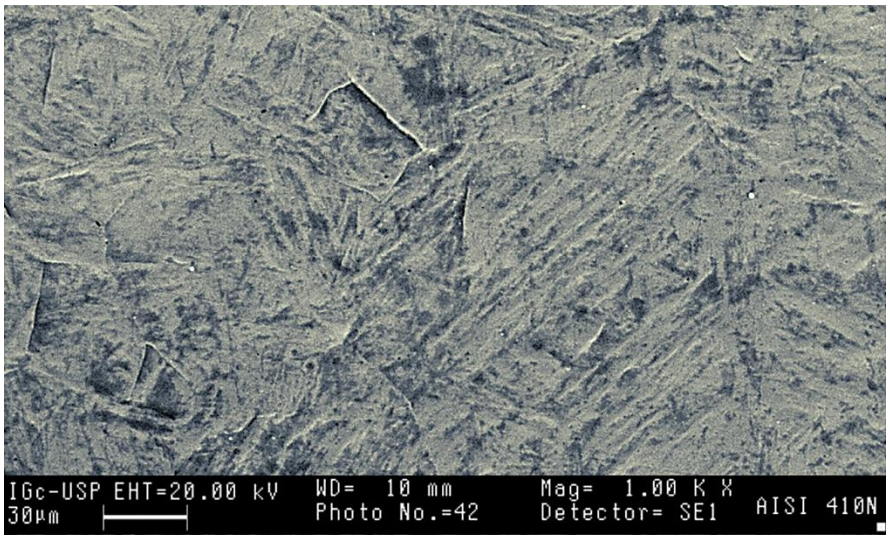

Fig. 7. Micrograph of TMAZ of S3

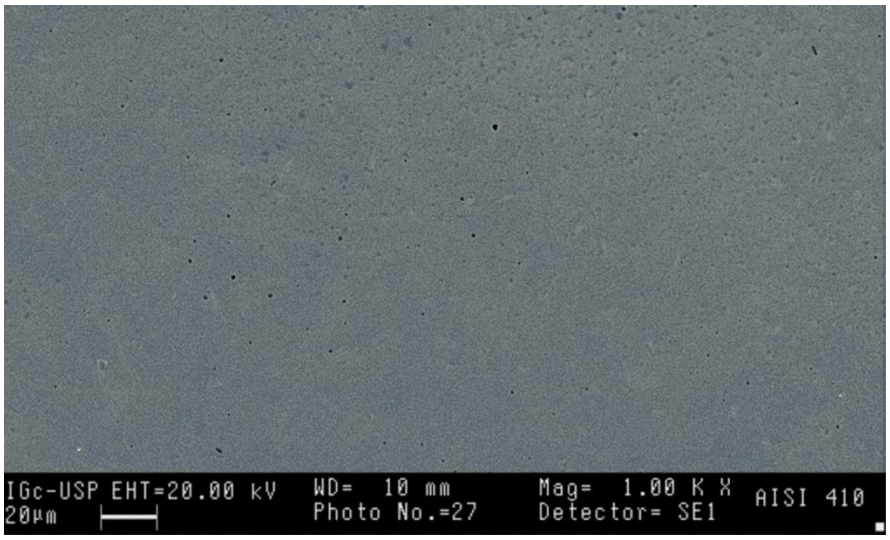

Fig. 8. Micrograph of SZ of S3

The above micrographs show that the morphology of the specimen is alike. That means the stir zone has the homogeneous finest grain structure due to the plastic deformation by the tool and the in-situ heating; thus, fine grain structure recrystallization will happen. Moreover, the grain size will depend on the degree of deformation, which means the grain size will reduce according to the increase in plastic deformation. Coarse grains are visible in the heat-affected zone, and the thermomechanical affected area reveals the deformed grains [51,52]. The thermomechanical region's grain size is slightly larger than the stir zone due to the heat generated in that region being inadequate for recrystallization. In this TMAZ region, the deformed grain structure was visible due to the plastic deformation with the tool pin rotation [53]. The grain growth was observed in the heat-affected zone too, this was hopping due to the frictional heat and in situ heat generated by the tool shoulder, pin and induction heating coil.

Also, IA-FSW's influence on the AISI 410 stainless steel joint's microstructural features was analyzed using SEM and EDX. Figure 9 shows the SEM image of IA-FSW specimens stir zone with twinning [54,55]. Figure 10 shows the EDX elemental profile across the IA-FSW joint.

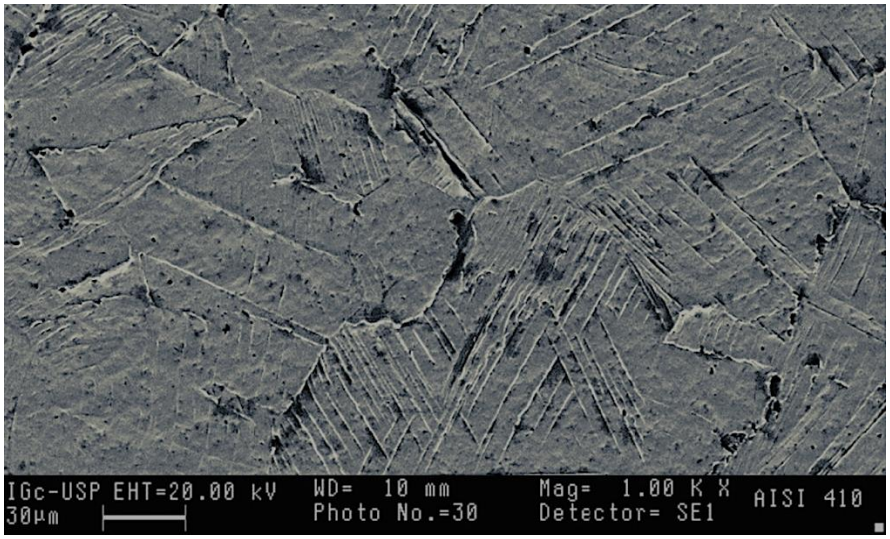

Fig. 9. Stir zone twinning

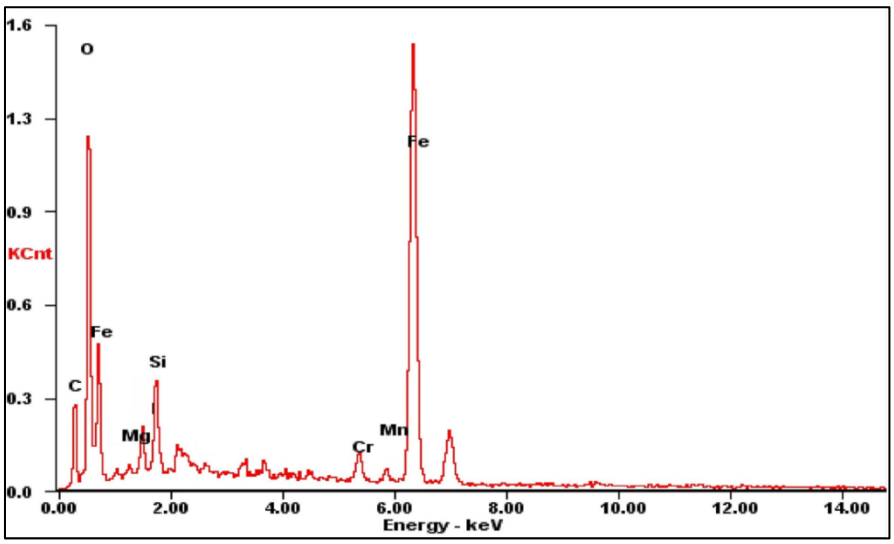

Fig. 10. EDX analysis across the IA-FSW joint

The metal movement in the stir zone is shown in Figure 8. The structural transformation in martensitic steel is very rapid while in the joining process. As a result of this rapid transformation, the carbon content will be trapped, and the remaining particle in this region was carbide alone [56]. Due to this process, a few carbide quantities will always be visible in the IA-FSW joints' stir zone. Some scatter was visible in the stir zone; this was happening with the tool pin rotation in the stir zone.

The EDX analysis across the induction-assisted friction stir welded AISI 410 stainless steel are shown in Figure 9. The EDX analysis reveals that scatter has occurred in the merging area of the martensitic and ferritic region, resulting from low stacking fault energy [57]. Due to recrystallization happening in the stir zone, a refined grain structure was achieved, enhancing the corrosion resistance of the specimen. In future, the same method will be adopted to investigate the mechanical properties and metallurgical properties of similar and dissimilar metal joints. The joints produced by conventional FSW also show better corrosion resistance, while the addition of in-situ induction heating enhances the corrosion rate in martensitic steel.

CONCLUSIONS

In this research, AISI 410 stainless steel was joined using a novel induction assisted friction stir welding (IA-FSW) method. The effect and influence of IA-FSW microstructure and corrosive behaviour were investigated. The findings are given below.

1) The best parameter combination was found out for conducting IA-FS welding on AISI 410 SS without any defects. The optimum parameter combination for joining AISI 410 SS is spindle speed 1150 rpm, welding speed 40 mm/min, plunge depth 0.5 mm, and in-situ heat 480ºC at 40W.
2) The specimen S3, which was welded using the optimum parameter combinations, achieved the highest corrosion resistance property, comparatively higher than other joints configurated. The corrosion rate for 1 M HCL was 1.80600 mm/year for the 3-hour test and 1.82017 mm/year for the 24-hour test.
3) Specimen S3 shows a homogenous fine grain structure; this was achieved using proper spindle speed, welding speed and in situ heat input to attribute appropriate recrystallization.

REFERENCES

1. Siddiquee AN, Pandey S, Khan NZ: Friction Stir Welding of austenitic stainless steel: a study on microstructure and effect of parameters on tensile strength. Materials Today: Proceedings, 2, 2015, 1388-1397.
2. Mohan DG, Gopi S, Rajasekar V: Effect of induction assisted friction stir welding on corrosive behaviour, mechanical properties and microstructure of AISI 410 stainless steel. Indian Journal of Engineering and Materials Sciences, 25, 2018, 203-208.
3. Astarita A, Curioni M, Squillace A, Zhou X, Bellucci F, Thompson GE, Beamish KA: Corrosion behaviour of stainless steel–titanium alloy linear friction welded joints: Galvanic coupling. Materials and Corrosion, 66(2), 2018, 111-117.
4. Atapour M, Sarlak H, Esmailzadeh M: Pitting corrosion susceptibility of friction stir welded lean duplex stainless steel joints. International Journal of Advanced Manufacturing Technologies, 83, 2015, 721-728.
5. Skowrońska B, Chmielewski T, Kulczyk M, Skiba J, Przybysz S: Microstuctural investigation of a friction-welded 316L stainless steel with ultrafine-grained structure obtained by hydrostatic extrusion. Materials, 14(6), 2021, 1537.
6. Chen J, Shi L, Wu CS, Jiang Y: The effect of tool pin size and taper angle on the thermal process and plastic material flow in friction stir welding. International Journal of Advanced Manufacturing Technology, 116, 2021, 2847–2860.
7. Mohan DG, Gopi S, Sasikumar A: Examining the mechanical and metallurgical properties of single pass friction stir welded dissimilar aluminium alloys tee joints. SVOA Materials Science & Technology, 3(1), 2021, 6–12.
8. Chagas de Souza G, da Silva AL, Tavares SSM, Pardal JM, Ferreira MLR, Filho IC: Mechanical properties and corrosion resistance evaluation of super duplex stainless steel UNS S32760 repaired by GTAW process. Welding International, 30, 2016, 432–442.

9. Mohan DG, Gopi S: Study on the mechanical behaviour of friction stir welded aluminium alloys 6061 with 5052. The 8th Industrial Automation and Electromechanical Engineering Conference, Institute of Engineering and Management, Bangkok, Thailand, 2017.
10. Mohan DG, Wu CS: A Review on Friction Stir Welding of Steels. Chinese Journal of Mechanical Engineering, Springer, 2021 (In press)
11. Guo R, Shen Y, Huang G, Zhang W, Guan W: Microstructures and mechanical properties of thin 304 stainless steel sheets by friction stir welding. Journal of Adhesion Science and Technology, 32(12), 2018, 1313-1323.
12. Subramanian K, Murugesan S, Mohan DG, Tomków J. Study on Dry Sliding Wear and Friction Behaviour of Al7068/Si3N4/BN Hybrid Composites. Materials, 14, 2021, 6560.
13. Kubit A, Drabczyk M, Trzepieciński T, Bochnowski W, Kaščák Ľ, Slota J: Fatigue life assessment of refill friction stir spot welded alclad 7075-T6 aluminium alloy joints. Metals, 10, 2020, 633.
14. Song G, Li T, Yu J, Liu L: A review of bonding immiscible Mg/steel dissimilar metals. Materials, 11, 2018, 2515.
15. Liu FC, Hovanski Y, Miles MP, Sorensen CD, Nelson TW: A review of friction stir welding of steels: Tool, material flow, microstructure, and properties. Journal of Materials Science & Technology, 34(1), 2018, 39-57.
16. Mohan DG, Gopi S, Rajasekar V: Mechanical and corrosion resistant properties of hybrid-welded stainless steel. Materials Performance, 57(1), 2018, 53–56.
17. Tamadon A, Pons DJ, Sued K, Clucs D: Internal flow behaviour and microstructural evolution of the bobbin-FSW welds: Thermomechanical comparison between 1XXX and 3XXX aluminium grades. Advances in Materials Science, 21(2), 2021, 40-64.
18. Cui L, Zhang C, Yong-chang L, Liu XG, Wang DP, Li HJ: Recent progress in friction stir welding tools used for steels. Journal of Iron and Steel Research International, 25, 2018, 477-486.
19. Gao S, Zhao H, Zhang R, Ma C, Zhou L, Chen G, Li D, Yang H, Song X, Zhao Y: Microstructure evolution of friction stir processed 2507 duplex stainless steel. Welding in the World, 2021.
20. Han Y, Jiang X, Chen S, Yuan T, Zhang H, Bai Y, Xiang Y, Li X: Microstructure and mechanical properties of electrically assisted friction stir welded AZ3 1B alloy joints. Journal of Manufacturing Processes, 43, 2019, 26-34.
21. Gopi S, Manonmani, K: Predicting tensile strength of double side friction stir welded 6082-T6 aluminium alloy. Science and Technology of Welding and Joining, 17(7), 2012, 601-607.
22. Hua P, Moronov S, Nie CZ, Sato YS, Kokawa H, Park SHC, Hirano S: Microstructure and properties in friction stir weld of 12Cr steel. Science and Technology of Welding and Joining, vol. 19, 2014, 176- 181.
23. Mohan DG, Gopi S: Influence of In-situ induction assisted friction stir welding on tensile, microhardness, corrosion resistance and microstructural properties of martensitic steel. Engineering Research Express, 3, 2021, 025023.
24. Cui L, Fujii H, Tsuji N, Nogi K: Friction stir welding of a high carbon steel. Scripta Materialia, 56, 2017, 637-640.
25. Magnani M, Terada M, Lino AO, Tallo VP, da Fonseca EB, Santos TFA, Ramirez AJ: Microstructural and electrochemical characterization of friction stir welded duplex stainless steels. International Journal of Electrochemical Science, 9, 2014, 2966- 2977.
26. Mohan DG, Gopi S: Induction assisted friction stir welding: a review. Australian Journal of Mechanical Engineering, 1, 2018, 119-123.

27. Mironov S, Sato YS, Yoneyama S, Kokawa H, Fujii HT, Hirano S: Microstructure and tensile behavior of friction-stir welded TRIP steel. Materials Science and Engineering A, 717, 2018, 72-82.
28. Wang L, Chen J, Wu CS: Auxiliary energy-assisted arc welding processes and their modelling, sensing and control. Science and Technology of Welding and Joining, 26(5), 2021, 389-411.
29. Thimmaraju PK, Arakanti K, Chandra Mohan Reddy G: Influence of tool geometry on material flow pattern in friction stir welding process. International Journal of Theoretical and Applied Mechanics, 12, 2017, 445-458.
30. Memon S, Paidar M, Sadreddini S, Cooke K, Babaei B, Ojo OO: Mechanical and microstructural aspects of the hybrid joint of PP-C30S and 2219 aluminum alloy. Results in Physics, 19, 2020, 103629.
31. Sasikumar A, Gopi S, Mohan, DG: Effect of magnesium and chromium fillers on the microstructure and tensile strength of friction stir welded dissimilar aluminium alloys. Materials Research Express, 6(8), 2019, 086580.
32. Shrikrishna KA, Sathiya P: Effects of post weld heat treatment on friction welded duplex stainless steel joints. Journal of Manufacturing Processes, 21, 2015, 196–200.
33. Li X, Li C, Liang Z, Xusheng Q, Wang D: Research on the corrosion behavior of double-side friction stir welded 6082Al alloy thick plate. Journal of Adhesion Science and Technology, 35(9), 2020, 993-1005.
34. Su H, Wang T, Wu CS. Formation of the periodic material flow behaviour in friction stir welding, Science and Technology of Welding and Joining, 26(4), 2021, 286-293.
35. Yang C, Wu C, Gao S. Modified constitutive equation by using phase field simulation of dynamic recrystallization in friction stir welding. Journal of Materials Research and Technology, 12, 2021, 916–929.
36. Paidar M, Memon S, Samusenkov VO, Babaei B, Ojo OO: Friction spot extrusion welding-brazing of copper to aluminum alloy. Materials Letters, 285, 2021, 129160.
37. Walczak M, Szala M: Effect of shoot peening on the surface properties, corrosion and wear performance of 17-4PH steel produced by DMLS additive manufacturing. Archives of Civil and Mechanical Engineering, 21, 2021, 157.
38. Guo C, Shen Y, Hou W, Yan Y, Huang G, Liu W: Effect of groove depth and plunge depth on microstructure and mechanical properties of friction stir butt welded AA6061-T6. Journal of Adhesion Science and Technology, 32(24), 2018, 2709-726.
39. Sun Z, Wu C S. Influence of tool thread pitch on material flow and thermal process in friction stir welding. Journal of Materials Processing Technology, 275, 2020,116281.
40. Mohan DG, Tomków J, Gopi S: Induction assisted hybrid Friction Stir Welding of dissimilar materials AA5052 aluminium alloy and X12Cr13 stainless steel. Advances in Materials Science, 21(3), 2021, 17-30.
41. Memon S, Paidar M, Mehrez S, Cooke K, Ojo OO, Lankarani HM: Effects of materials positioning and tool rotational speed on metallurgical and mechanical properties of dissimilar modified friction stir clinching of AA5754-O and AA2024-T3 sheets. Results in Physics, 22, 2021, 103962.
42. AnandhaKumar CJ, Gopi S, Mohan DG, Shashi Kumar S: Predicting the ultimate tensile strength and wear rate of aluminium hybrid surface composites fabricated via friction stir processing using computational Mmethods. Journal of Adhesion Science and Technology, 2021.
43. Balamurugan M, Gopi S, Mohan DG: Influence of tool pin profiles on the filler added friction stir spot welded dissimilar aluminium alloy joints. Materials Research Express, 8, 2021, 096531.

44. Memon S, Fydrych D, Fernandes AC, Derazkola HaA, Derazkola HeA: Effect of FSW tool plunge depth on properties of an Al-Mg-Si alloy T-joint: thermomechanical modelling and experimental evolution. Materials, 14, 2021, 4754.

45. Gopi S, Mohan DG: Evaluating the welding pulses of various tool profiles in single-pass friction stir welding of 6082-T6 aluminium alloy. Journal of Welding and Joining, The Korean Welding and Joining Society, 39(3), 2021, 284-294.

46. Memon S, Paidar M, Ojo OO, Cooke K, Babaei B, Masoumnezhad M: The role of stirring time on the metallurgical and mechanical properties during modified friction stir clinching of AA6061-T6 and AA7075-T6 sheets. Results in Physics, 19, 2020, 103364.

47. Sasikumar A, Gopi S, Mohan DG: Effect of welding speed on microhardness and corrosion resistance properties of filler induced friction stir welded AA6082 and AA5052 joints. Materials Research Express, 8, 2021, 066531.

48. Geng X, Feng H, Jiang Z, Li H, Zhang B, Zhang S, Wang Q, Li J: Microstructure, mechanical and corrosion properties of friction stir welding high nitrogen martensitic stainless steel 30Cr15Mo1N. Metals, 6(12), 2016, 301.

49. Mohan DG, Gopi S: Influence of in-situ induction heated friction stir welding on tensile, microhardness, corrosion resistance and microstructural properties of martensitic steel. Engineering Research Express, 3, 2021, 025023.

50. Memon S, Paidar M, Mehta KP, Babaei B, Lankarani HM: Friction spot extrusion welding on dissimilar materials AA2024-T3 to AA5754-O: effect of shoulder plunge depth. Journal of Materials Engineering and Performance, 30, 2021, 334-345.

51. Mohan DG, Gopi S: Optimized parameters prediction for single-pass friction stir welding on dissimilar aluminium alloys T-joint. International Journal on Emerging Technologies, 12(2), 2021, 15-20.

52. Yu X, Mazumder B, Miller MK, David S, Feng Z: Stability of Y–Ti–O precipitates in friction stir welded nanostructured ferritic alloys. Science and Technology of Welding and Joining, 20, 2015, 236-241.

53. Ghiasvand A, Yavari MM, Tomków J, Grimaldo Guerrero JW, Kheradmandan H, Dorofeev A, Memon S, Derazkola HA: Investigation of mechanical and microstructural properties of welded specimens of AA6061-T6 alloy with friction stir welding and parallel-friction stir welding methods. Materials, 14, 2021, 6003.

54. Kosturek R, Śnieżek L, Torzewski J, Ślęzak T, Wachowski M, Szachogłuchowicz I: Research on the properties and low cycle fatigue of Sc-modified AA2519-T62 FSW joint. Materials, 13, 2020, 5226.

55. Sameer MD, Birru AK: Selection of friction stir welding tool rotational speed for joining dual phase DP600 steel sheets – an experimental approach. Journal of Adhesion Science and Technology, 35, 2020, 751-776.

56. Liu XC, Sun YF, Nagira T, Ushioda K, Fujii H: Microstructure evolution of Cu–30Zn during friction stir welding. Journal of Materials Science, 53, 2018, 10423-10441.

57. Paidar M, Mehrez S, Babaei B, Memon S, Ojo OO, Lankarani HM. Dissimilar welding of AA5083 to AZ31 Mg alloys using modified friction stir clinching brazing. Materials Letters, 301, 2021, 129764.